

Three-dimensional tissue culture based on magnetic cell levitation

Glauco R. Souza^{1†}, Jennifer R. Molina², Robert M. Raphael³, Michael G. Ozawa¹, Daniel J. Stark⁴, Carly S. Levin⁵, Lawrence F. Bronk¹, Jeyarama S. Ananta⁶, Jami Mandelin¹, Maria-Magdalena Georgescu², James A. Bankson⁷, Juri G. Gelovani⁸, T. C. Killian^{4*}, Wadih Arap^{1*} and Renata Pasqualini^{1*}

Cell culture is an essential tool in drug discovery, tissue engineering and stem cell research. Conventional tissue culture produces two-dimensional cell growth with gene expression, signalling and morphology that can be different from those found *in vivo*, and this compromises its clinical relevance^{1–5}. Here, we report a three-dimensional tissue culture based on magnetic levitation of cells in the presence of a hydrogel consisting of gold, magnetic iron oxide nanoparticles and filamentous bacteriophage. By spatially controlling the magnetic field, the geometry of the cell mass can be manipulated, and multicellular clustering of different cell types in co-culture can be achieved. Magnetically levitated human glioblastoma cells showed similar protein expression profiles to those observed in human tumour xenografts. Taken together, these results indicate that levitated three-dimensional culture with magnetized phage-based hydrogels more closely recapitulates *in vivo* protein expression and may be more feasible for long-term multicellular studies.

Although protein-based gel environments or rotational/agitation-based bioreactors have been developed in attempts to allow three-dimensional cell culture^{1–5}, broad practical application of such methods has not yet been achieved^{2–4}. A straightforward technology enabling three-dimensional cell culture therefore remains an unmet need^{3,4}. To address this challenge, we introduce a ‘three-dimensional bio-assembler’ that relies on magnetic forces and cell levitation^{6–8}. The methodology is based on the cellular uptake and subsequent magnetic levitation of a bioinorganic hydrogel composed of bacteriophage (phage) plus magnetic iron oxide (MIO; Fe₃O₄, magnetite) and gold nanoparticles that self-assemble into hydrogels (Fig. 1a). Incorporation of MIO nanoparticles creates a new material that retains the biocompatibility of gold–phage hydrogels^{9,10} while adding capabilities for the culture and magnetic manipulation of cells.

The technology reported here provides an alternative to biodegradable porous scaffolds and protein matrices^{11,12}. In general, biodegradable scaffolds may suffer from slow or delayed propagation of cells and establishment of cell–cell interactions. Existing commercial products, such as Matrigel¹¹, are useful and not particularly expensive, but their chemical composition is fixed (that is, unchangeable). In contrast, our bio-assembler allows adaptable magnetic-based cell levitation and may provide for improved three-dimensional cell-growth conditions in certain settings. The methodology is

cost-effective, because it does not require a specific medium, and it is compatible with standard two-dimensional cell culture techniques.

The biological application of magnetic forces has long been studied^{13–18}. For example, magnetic resonance imaging is a mainstay of clinical diagnostic radiology, relying on superconducting magnets and large magnetic fields. Magnets have also been used to levitate biological samples through the natural diamagnetism of organic materials⁶. Incorporation of MIO nanoparticles has further enabled manipulation of surface patterns^{7,13}, contrast-enhanced magnetic resonance imaging¹⁴, cell sorting¹⁴, mechano-conditioning of cells^{14–16}, studies of mechano-sensitive membrane properties¹⁷, and cellular micromanipulation¹⁸. However, although MIO nanoparticles can be modified to target proteins or can be coupled to cationic liposomes for delivery and concentration¹³, the combination of ligand peptide-mediated targeting and magnetic levitation to achieve three-dimensional cell culture has not yet been systematically applied.

Our hydrogel uses M13-derived phage particles, displaying the ligand peptide CDCRGDCFC (termed RGD-4C) to target α v integrins^{19,20}, gold nanoparticles and MIO. Phage are being investigated for biotechnological and materials applications²¹ such as targeted gene delivery²⁰, optical imaging microscopy⁹ and protein targeting¹⁹. Both phage and gold nanoparticles are potentially biocompatible and have even been approved by the United States Food and Drug Administration for use in several applications²². Under the conditions used, MIO nanoparticles are well-tolerated by mammalian cells, a result consistent with previous reports^{7,13,23}. Magnetic-based levitation of cell-targeted hydrogels may therefore become a useful biotechnology tool.

To first evaluate and then confirm the presence of MIO in the hydrogels, we applied several methodologies, including elastic light scattering, magnetic resonance imaging and inductively coupled plasma atomic emission spectroscopy (Fig. 1b–d, see also Supplementary Figs S1,S2). Having demonstrated the presence of MIO within the targeted hydrogel, we subsequently used murine C17.2 neural stem cells²⁴ to evaluate the ability of the system to induce magnetic field-based cell levitation (Fig. 2). The admixture of neural stem cells and MIO-containing hydrogel co-rose to the air–medium interface, but was unable to leave the medium, presumably due to surface tension (Fig. 2a–c). The observed cell levitation in the liquid medium confirms that the field from a permanent magnet is sufficient to overcome the gravitational force to reach a steady state, consistent with our theoretical estimates

¹David H. Koch Center, The University of Texas M.D. Anderson Cancer Center, Houston, Texas 77030, USA, ²Department of Neuro-Oncology, The University of Texas M.D. Anderson Cancer Center, Houston, Texas 77030, USA, ³Department of Bioengineering, Rice University, Houston, Texas 77005, USA, ⁴Department of Physics and Astronomy, Rice University, Houston, Texas 77005, USA, ⁵Nano3D Biosciences, Inc., Houston, Texas 77030, USA, ⁶Department of Chemistry, Rice University, Houston, Texas 77005, USA, ⁷Department of Imaging Physics, The University of Texas M.D. Anderson Cancer Center, Houston, Texas 77030, USA, ⁸Department of Experimental Diagnostic Imaging, The University of Texas M.D. Anderson Cancer Center, Houston, Texas 77030, USA; [†]Present address: Nano3D Biosciences, Inc., Houston, Texas 77030, USA. *e-mail: killian@rice.edu; warap@mdanderson.org; rpsqual@mdanderson.org

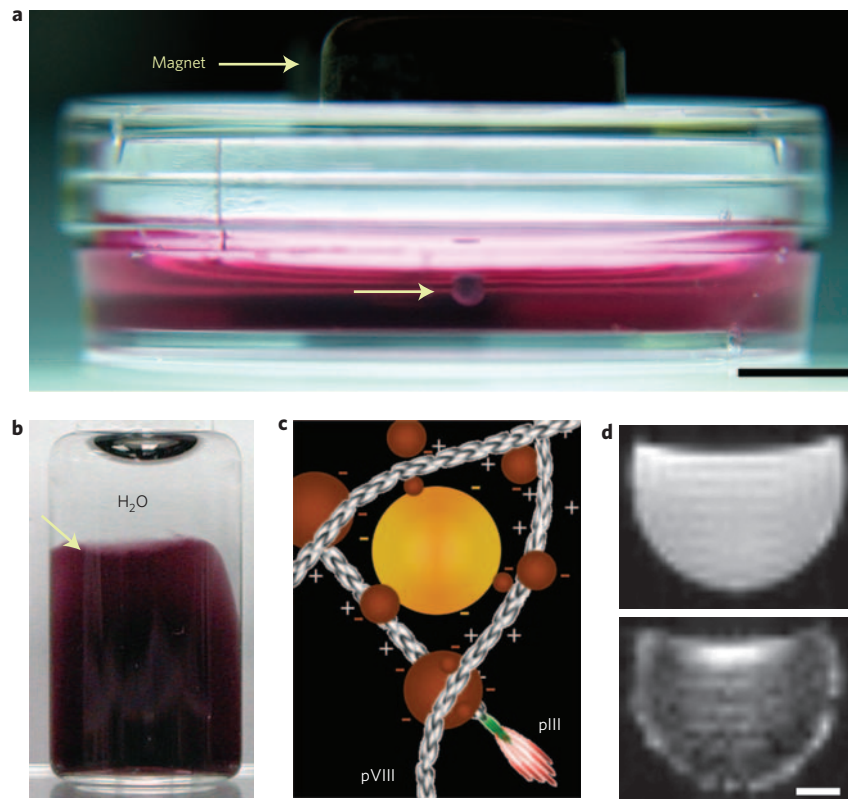


Figure 1 | Magnetic iron oxide-containing hydrogels. **a**, Human glioblastoma cells (lower arrow) treated with magnetic iron oxide (MIO)-containing hydrogel held at the air-medium interface by a magnet. The image was captured at 48 h of culture and depicts a ~ 1 -mm spheroid. Scale bar, 5 mm. **b**, Vial of a MIO-containing hydrogel (arrow) in water. **c**, Scheme of electrostatic interactions of MIO (brown spheres) and gold (yellow spheres) nanoparticles with phage (elongated structures; pIII and pVIII indicate surface capsid proteins). Nanoparticles are not drawn to scale. **d**, MRI image (T_2^* -weighted) of purified hydrogel in solution: MIO-free hydrogel control (top panel), average $T_2^* = 46.2$ ms; MIO-containing hydrogel (bottom panel), average $T_2^* = 16$ ms. Scale bar, 2 mm.

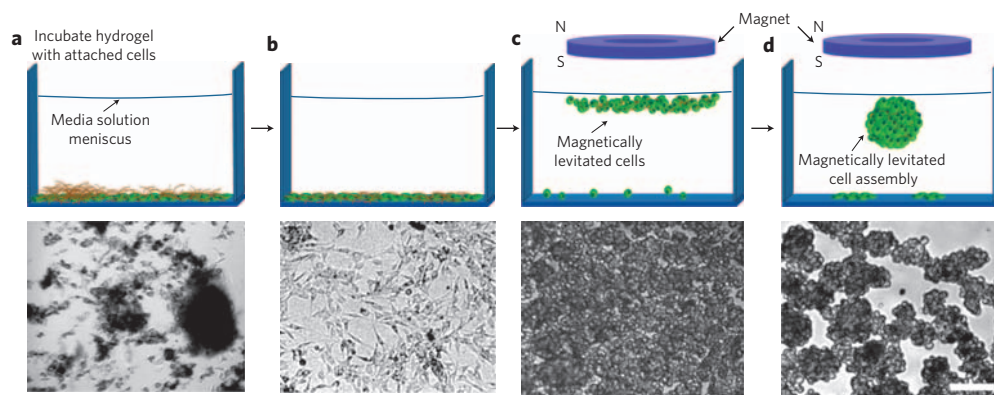


Figure 2 | Three-dimensional cell culture with magnetic-based levitation. The top row shows the general cell levitation strategy and the bottom row shows the corresponding optical micrograph of neural stem cells at each stage. **a**, Hydrogel is dispersed over cells and the mixture is incubated. The dark blotches are fragments of hydrogel. **b**, Washing steps remove non-interacting hydrogel fragments. Fractions of phage, gold and MIO nanoparticles enter cells or remain membrane-bound. **c**, Application of an external magnet causes cells to rise to the air-medium interface. The image shows culture 15 min after levitation. **d**, After 12 h of levitation, characteristic multicellular structures form (a single structure is shown in the schematic). Scale bar (bottom row), 30 μm .

(Supplementary Fig. S3). Although the liquid-air interface could also be regarded as a physical barrier for levitated cell culture, it lacks a solid material surface for cell attachment and growth. We observed that the magnetic field concentrated clusters of levitated cells in solution, triggering cell-cell interactions in a manner consistent with tissue engineering scaffolds³ designed to bestow cell growth advantage. In general, three-dimensional cell cultures were axially symmetric and, on a large scale, reflected the symmetry of

the magnets used. However, under magnification, we observed small-scale multicellular assembly features (Fig. 2d) with characteristic and reproducible branching morphogenesis²⁵.

To assess cell growth within the bio-assembler, we visually and quantitatively monitored the formation rate, size and viability of genetically modified human glioblastoma cells over a period of 8 d by monitoring the fluorescence from stable protein expression of mCherry (Fig. 3a). Within 30 min of levitation, cells were

brought together (Fig. 3a, 0.5 h); moreover, a cohesive multicellular assembly emerged by 24 h and a spheroid shape formed between 72 h and 192 h, reaching a maximum diameter of ~ 1 mm. We obtained similar results—albeit with a lower initial yield—with a shorter incubation of the cells and MIO-containing hydrogels (Supplementary Fig. S4).

Morphological analysis of the architectural integrity of three-dimensional structures was also performed with transmission and scanning electron microscopy. In ‘small’ spheroids, we noted viable cells throughout the structure. In contrast, in ‘large spheroids’ we observed central necrosis surrounded by a viable outer region (Supplementary Figs S5–S7). Although such features may in fact be desirable in emulating conditions within the tumour microenvironment (such as ischaemia, acidosis or nutrient transport, among other parameters), the formation of a heterotypic vascular supply from exogenous angiogenic endothelial cells is an active area of research and development. Together, future use of serial co-cultures of endothelium-derived cells and different ligand peptides or varying magnetic fields can also be envisioned.

The intense red fluorescence from mCherry protein expression confirmed cell viability within the three-dimensional assembly, and cultures could be maintained for at least 12 weeks, at which time the experiment was terminated (Supplementary Fig. S8). We compared the growth rate of magnetically levitated cells with that of cells in standard two-dimensional cultures (Fig. 3b). In contrast to the indicated exponential trend for the growth of levitated cells, cell culture in two dimensions showed a linear growth pattern, a feature of surface attached cultures²⁶. Because of the volume accessible during three-dimensional growth, a large assembly can be accomplished without the de-attachment/re-plating cycles (‘passage’) required in standard tissue culture.

To explore the biological attributes afforded by magnetic levitation in our system, we cultured human glioblastoma cells and observed not only morphological but also molecular similarity to orthotopic human tumour xenografts from immunodeficient mice (Fig. 3c). We evaluated the marker N-cadherin, a transmembrane protein mediating cell–cell contact through homotypic cell adhesion interactions²⁷. N-cadherin expression in three-dimensional cultures

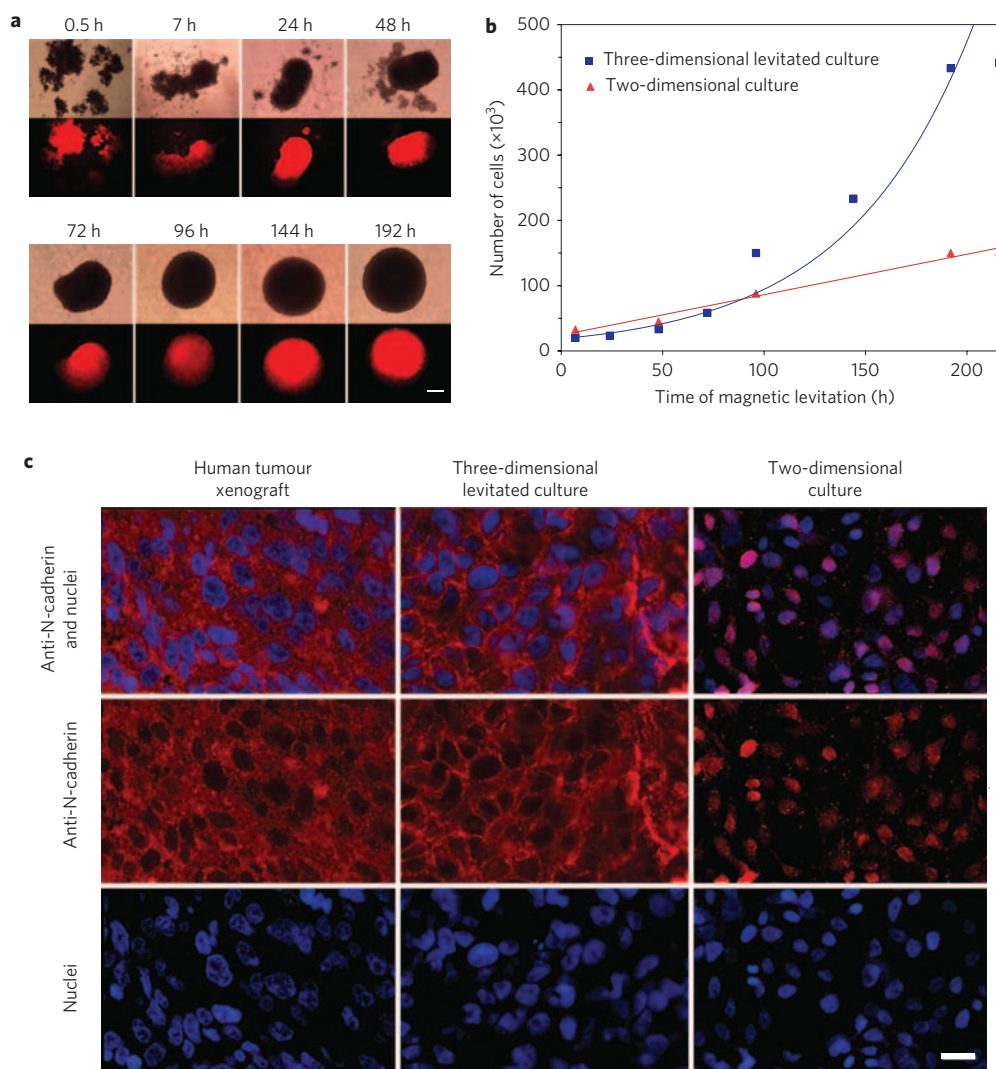


Figure 3 | Comparison of three-dimensional cell growth with standard two-dimensional tissue culture. a, Phase contrast (top row) and fluorescence (mCherry; bottom row) images of levitated human glioblastoma cells monitored over eight days. Cells coalesced within hours and formed spheroids by 24 h. Scale bar, 200 μ m. **b**, Number of cells as a function of time for levitated cell culture (blue squares) and representative two-dimensional culture (red triangles). Line fits indicate an exponential trend for levitated cells (blue line) and linear trend for surface attached cells (red line). **c**, Immunofluorescence detection of N-cadherin (red) and DAPI nuclear staining (blue) in a mouse xenograft, three-dimensional magnetic levitation for 48 h, and two-dimensional standard culture for 48 h with human glioblastoma cells. Scale bar, 10 μ m.

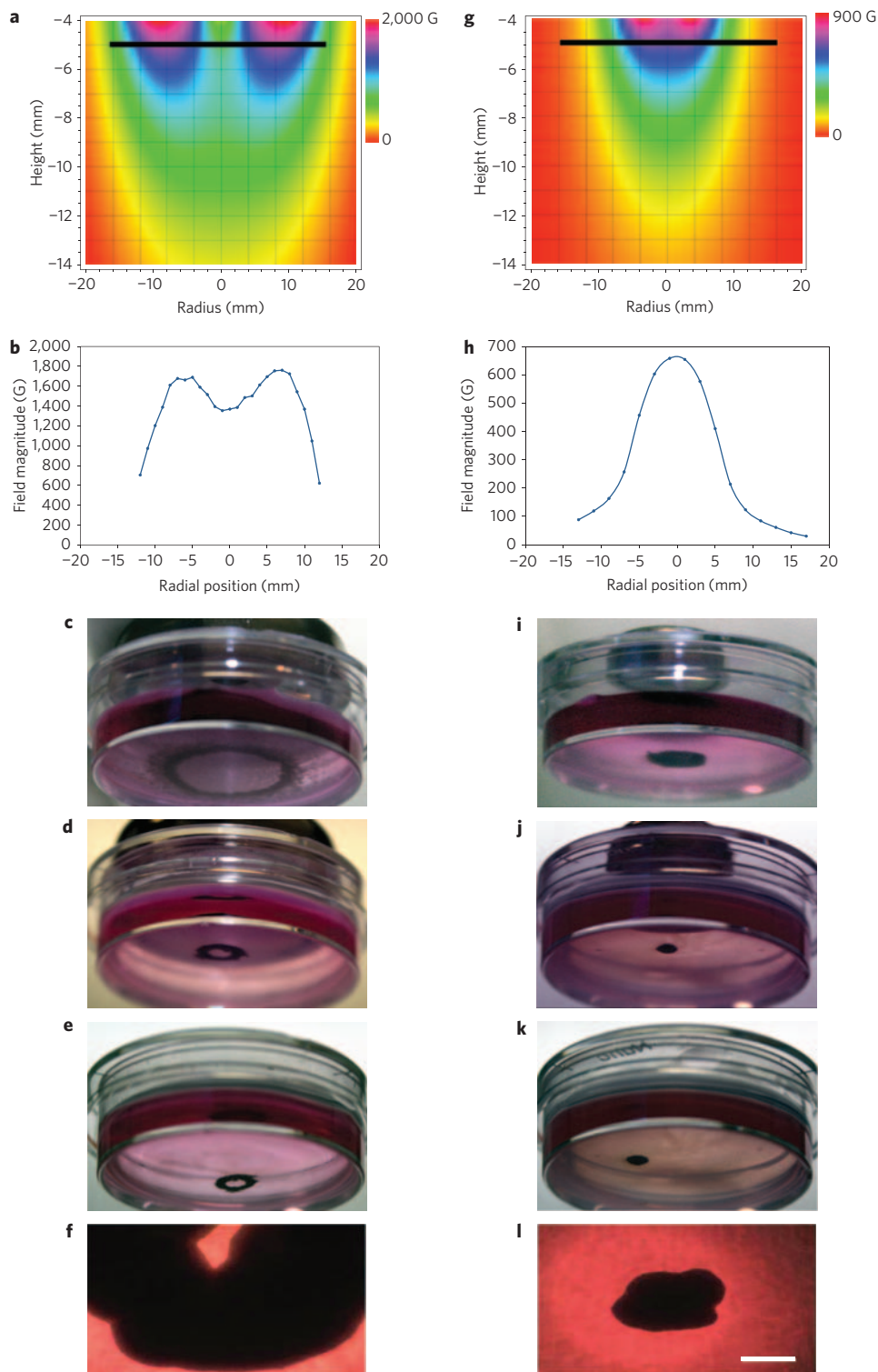


Figure 4 | Shape control of magnetically levitated culture. Three-dimensional culture derived from magnets with outer radii of 12 mm (a-f) and 6 mm (g-l). a,g, Estimated magnetic field profiles obtained by direct integration of the Biot-Savart law using Mathematica (see Supplementary Information). b,h, Hall probe measurements along a diameter perpendicular to the symmetry axis at the air-medium interface. Lines are spline fits. c-e,i-k, Human glioblastoma cells at the onset of levitation (c,i), 30 h (d,j) and following magnet removal at 30 h (e,k). f,l, Spheroid images after growth for one week. Scale bar, 400 μm.

suggests that magnetic levitation may recapitulate at least some *in vivo*-like traits. Indeed, two-dimensional cultures show N-cadherin scattered in the cytoplasm and nucleus but absent from the membrane, whereas three-dimensional-levitated cells express N-cadherin in the membrane, cytoplasm and cell junctions (akin to the protein expression pattern observed in tumour xenografts).

Our results are qualitatively consistent with those recently reported by Ofek and colleagues²⁷ in which cartilage grown *in vitro* also yielded differential N-cadherin expression patterns in three-dimensional relative to two-dimensional culture. In control experiments, we observed no alterations in N-cadherin expression under conditions including (1) MIO-containing hydrogels with no magnetic

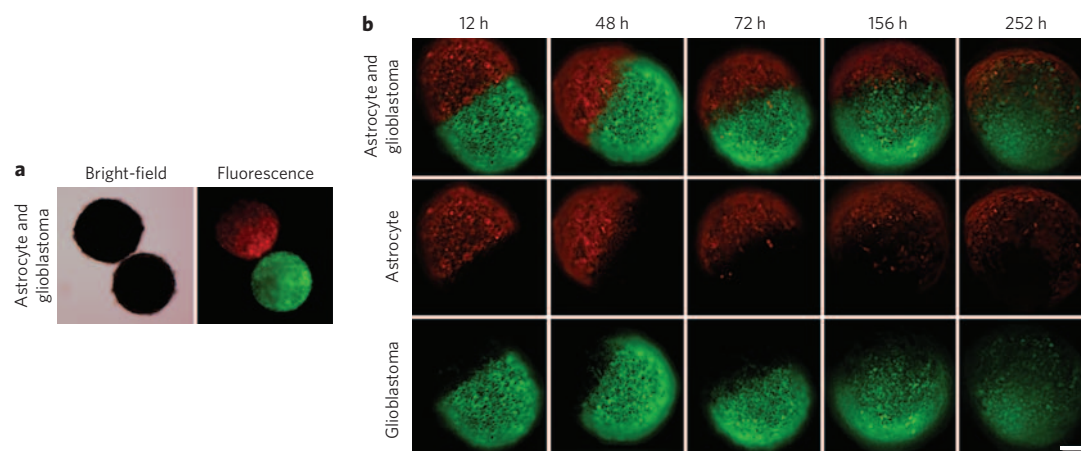


Figure 5 | Confrontation assay of magnetically levitated multicellular spheroids. **a**, Bright-field and fluorescence images of human glioblastoma cells (green; GFP-expressing cells) and normal human astrocytes (red; mCherry-labelled) cultured separately and then magnetically guided together (time = 0). **b**, Confrontation between human glioblastoma cells and normal astrocytes monitored for 10.5 d. Invasion of the spheroid composed of normal human astrocytes by human glioblastoma cells serves as a standard assay of glioma invasiveness²⁹. Scale bar, 200 μm .

field, (2) MIO-containing hydrogels with a magnetic field but cultured in two dimensions, and (3) cells alone under a magnetic field (Supplementary Fig. S9). Thus, magnetically induced three-dimensional tissue culture *in vitro* may become a complementary and cheaper surrogate for the labour- and cost-intensive generation and maintenance of human brain tumour xenografts in immunodeficient mice.

To evaluate the ability of magnetic fields to provide a means to engineer cell culture shape, we levitated tumour cells with different ring-shaped magnets, assessed the magnetic field strength, and serially recorded culture morphology (Fig. 4). The resulting structures reflected the properties of the estimated (see Supplementary Information) and Hall probe measured magnetic field. For the large-radius magnet (Fig. 4a–f), the field at the height of the culture had a central minimum, which led to a ring-shaped cell pattern at the onset of levitation produced by the force pulling cells towards the field maximum (Fig. 4a,b); this shape persisted as cells assembled (Fig. 4c–f) and formed a cohesive structure with enough integrity to remain intact when the magnet was removed (Fig. 4e,f). Although ischaemia can cause central necrosis of spheroids cultured for long periods, the shape generated at the early time point was attributable to the magnetic field profile at the liquid–air interface. The small magnet produced a central maximum of the field at the height of the culture and a compact cellular assembly (Fig. 4g–l). In this initial work, the volume of medium and the magnetic fields were held constant, and volumetric variation did not adversely affect three-dimensional culture geometry.

Finally, magnetic field manipulation may provide precise temporal and/or spatial control of distinct cell populations in an environment conducive to visualization or molecular imaging *in situ*. We demonstrate the feasibility of confrontation assays with co-culture of human glioblastoma cells (GFP-transfected; Fig. 5, green cells) and normal human astrocytes (mCherry-transfected; red cells). Initially, a clear interface separating the cell structures was evident. By 12 h, the populations began to fuse and lose their individual spherical shapes. After 72 h, the populations coalesced into a single spheroid with the human glioblastoma cells invading the structure composed of normal human astrocytes. Glioblastoma is the most common, invasive and lethal type of astrocytic brain tumour²⁸, and these results illustrate the potential of this methodology for analysis of brain tumour invasiveness of normal brain in confrontation culture assays, which have been correlated with clinical outcome²⁹.

In conclusion, we have described a bio-assembler based on magnetic levitation with gold–phage–MIO as an enabling technology

for three-dimensional cell culture. We have demonstrated control of culture shape, and the ability to bring cultures together for controlled interaction in a confrontation assay with *in situ* monitoring. The magnetic levitation methodology reported here does not require a specific medium, engineered scaffolds, matrices or moulded gels. This simple, flexible and effective method may be suitable for a range of applications in biotechnology, drug discovery, stem cell research or regenerative medicine. Indeed, a potential long-term goal is the possibility of accomplishing the ‘engineering’ of normal tissues or complex organs¹². Side-by-side comparison with various other three-dimensional culture methods (including a panel of porous and biodegradable scaffolds) will ultimately determine the value of this technology in different experimental settings or applications.

Methods

Hydrogel self-assembly. Hydrogels were generated as described^{9,10} except for the inclusion of MIO nanoparticles. MIO-containing hydrogels were prepared by mixing the gold nanoparticle solution (optical absorbance, 530 nm = 1.2–1.5 units) with MIO nanopowder (magnetite [Fe₃O₄], polydisperse particle size <50 nm; stabilized with a surfactant of polyvinyl pyrrolidone; Sigma-Aldrich) to a concentration of 0.3 mg ml⁻¹. Magnetite nanoparticles were not placed in an oxidizing environment (chemical or heat) to avoid oxidation into another state such as maghemite [γ -Fe₂O₃]. Phage dilutions were prepared with 1×10^9 transducing units (TU) μl^{-1} in picopure water. Finally, the phage solution and the gold nanoparticle plus iron oxide solution were mixed with equal volumes and allowed to stand overnight at 4 °C for hydrogel formation.

Magnets. The ring-shaped, neodymium rare-earth magnets from Gaussboys (part nos MR32 and MR16) had outer (inner) radii of 12 (2.8) and 6 (1.7) mm, and thicknesses of 5 and 3 mm. Permanent magnetization was parallel to the symmetry axis.

Cell lines. Bosc, normal human astrocytes and human glioblastoma (LN-229 or U-251MG) cells were cultured in Dulbecco’s modified Eagle’s medium containing 10% fetal bovine serum (FBS). Transfections and retroviral infections were performed as described, and cells were selected and maintained with blasticidin (mCherry) or puromycin (eGFP) selection³⁰. C17.2 murine neural stem cells were cultured in high-glucose Dulbecco’s modified Eagle’s medium containing 10% FBS supplemented with sodium pyruvate 2 mM, glutamine, penicillin and streptomycin²⁴.

Magnetic levitation of cell culture in MIO-containing hydrogels. For levitated cell culture, surface attached cells (grown to ~80% confluence) were treated with 1 μl of hydrogel per 1 cm² of surface area available for cell culture and incubated overnight. Treated cells were de-attached by phosphate buffered saline (PBS) containing trypsin and EDTA and placed into a tissue culture Petri dish^{9,10}. A cover top with an attached neodymium magnet was immediately put in place. Trypan-blue excluding cells were de-attached and counted. Half of the sample (~3 $\times 10^4$ cells) was transferred to seed a two-dimensional surface-attached culture and the other half was seeded for a three-dimensional levitated culture.

Orthotopic glioma xenograft models. Human glioblastoma cells (2×10^6 cells per $10 \mu\text{l}$ of PBS; LN229 vector-GFP containing cells) were orthotopically implanted into the brains of immunodeficient (SCID) mice by direct intracranial injection at the right frontal lobe. Tumour-bearing mice were closely monitored and killed following any neurological signs of intracranial tumour burden. Tumour-containing brains were surgically collected and paraformaldehyde (PFA)-fixed for pathological analysis.

Immunofluorescence detection of N-cadherin. Human glioblastoma cells used for two-dimensional cell culture were prepared by first plating 1×10^5 cells on glass slides coated with poly-D-lysine and then allowing cells to attach overnight. Cells were subsequently washed with PBS and fixed with PBS containing 4% PFA for 30 min, and washed again. Cells were then permeabilized with PBS containing 0.1% triton X-100 for 5 min, washed with PBS, and treated with Image-iT FX signal enhancer (Invitrogen) for 30 min. Blocking was performed with PBS containing 0.2% gelatin and 10% donkey serum (PBS-gel) for 30 min. Three-dimensional cell structures from levitated cultures or brain xenografts were prepared with standard histopathology procedures. Briefly, three-dimensional structures were collected, washed twice in PBS, and fixed in PBS containing 4% PFA for 30 min, then washed again. Three-dimensional structures were subsequently embedded in paraffin blocks and sectioned. Samples were treated in xylene, hydrated through a series of ethanols (100%, 95%, 70%) and water. Samples were steamed in antigen retrieval solution (Dako) for 20 min, rinsed in water and transferred to PBS. Blocking was carried out with PBS containing 10% donkey serum for 30 min.

Microscope slides of the samples were incubated with primary antibody (anti-N-cadherin, Zymed) overnight in blocking buffer at 4°C . Cells were washed with PBS then treated with secondary antibody Alexa 488, 555 or 568 (Molecular Probes/Invitrogen) in PBS-gel for 1 h at room temperature. Cells were washed with PBS-gel then treated with DAPI in PBS-gel for 5 min, washed and mounted onto slides. Images (Z-stacks) were taken on a Zeiss deconvolution microscope and de-convolved with the Axiovert software.

Magnetic resonance measurements. MRI was acquired with a 4.7 T, 40 cm Bruker Biospec instrument. The MRI images were derived from a multi-gradient echo sequence with variance in $T2^*$ -weighting (500 ms repetition time, 16 echo times ranging from 1.5 to 39 ms, 64×64 image matrix, $32 \text{ mm} \times 32 \text{ mm}$ field of view). The characteristic time constant for exponential transverse signal decay ($T2^*$) was calculated from the average signal level of a region of interest in the centre of each phantom as a function of echo time. The image contrast between the MIO-containing hydrogel and the MIO-free control results from the reduction in $T2^*$ relaxation constant in the presence of iron oxide nanoparticles.

Received 26 October 2009; accepted 21 January 2010;
published online 14 March 2010

References

- Cukierman, E., Pankov, R., Stevens, D. R. & Yamada, K. M. Taking cell-matrix adhesions to the third dimension. *Science* **294**, 1708–1712 (2001).
- Abbott, A. Biology's new dimension. *Nature* **424**, 870–872 (2003).
- Pampaloni, F., Reynaud, E. G. & Stelzer, E. H. The third dimension bridges the gap between cell culture and live tissue. *Nature Rev. Mol. Cell Biol.* **8**, 839–845 (2007).
- Griffith, L. G. & Swartz, M. A. Capturing complex 3D tissue physiology *in vitro*. *Nature Rev. Mol. Cell Biol.* **7**, 211–224 (2006).
- Atala, A. Engineering tissues, organs and cells. *J. Tissue Eng. Regen. Med.* **1**, 83–96 (2007).
- Coleman, C. B. *et al.* Diamagnetic levitation changes growth, cell cycle and gene expression of *Saccharomyces cerevisiae*. *Biotechnol. Bioeng.* **98**, 854–863 (2007).
- Dobson, J. Remote control of cellular behaviour with magnetic nanoparticles. *Nature Nanotech.* **3**, 139–143 (2008).
- Ito, A., Shinkai, M., Honda, H. & Kobayashi, T. Medical application of functionalized magnetic nanoparticles. *J. Biosci. Bioeng.* **100**, 1–11 (2005).
- Souza, G. R. *et al.* Networks of gold nanoparticles and bacteriophage as biological sensors and cell targeting agents. *Proc. Natl Acad. Sci. USA* **103**, 1215–1220 (2006).
- Souza, G. R. *et al.* Bottom-up assembly of hydrogels from bacteriophage and Au nanoparticles: the effect of *cis*- and *trans*-acting factors. *PLoS ONE* **3**, e2242 (2008).
- Petersen, O. W., Ronnov-Jessen, L., Howlett, A. R. & Bissell, M. J. Interaction with basement membrane serves to rapidly distinguish growth and differentiation pattern of normal and malignant human breast epithelial cells. *Proc. Natl Acad. Sci. USA* **89**, 9064–9068 (1992).
- Mikos, A. G. *et al.* Engineering complex tissues. *Tissue Eng.* **12**, 3307–3339 (2006).
- Ito, A., Ino, K., Kobayashi, T. & Honda, H. The effect of RGD peptide-conjugated magnetite cationic liposomes on cell growth and cell sheet harvesting. *Biomaterials* **26**, 6185–6193 (2005).
- Pankhurst, Q., Connolly, J., Jones, S. K. & Dobson, J. Applications of magnetic nanoparticles in biomedicine. *J. Phys. D* **36**, R167–R181 (2003).
- Alsberg, E., Feinstein, E., Joy, M. P., Prentiss, M. & Ingber, D. E. Magnetically-guided self-assembly of fibrin matrices with ordered nano-scale structure for tissue engineering. *Tissue Eng.* **12**, 3247–3256 (2006).
- Dobson, J., Cartmell, S. H., Keramane, A. & El Haj, A. J. Principles and design of a novel magnetic force mechanical conditioning bioreactor for tissue engineering, stem cell conditioning and dynamic *in vitro* screening. *IEEE Trans. Nanobiosci.* **5**, 173–177 (2006).
- Meyer, C. J. *et al.* Mechanical control of cyclic AMP signaling and gene transcription through integrins. *Nature Cell Biol.* **2**, 666–668 (2000).
- Matthews, B. D., La Van, D. A., Overby, D. R., Karavitis, J. & Ingber, D. E. Electromagnetic needles with submicron pole tip radii for nanomanipulation for biomolecules and living cells. *Appl. Phys. Lett.* **85**, 2968–2970 (2004).
- Arap, W., Pasqualini, R. & Ruoslahti, E. Cancer treatment by targeted drug delivery to tumor vasculature in a mouse model. *Science* **279**, 377–380 (1998).
- Hajitou, A. *et al.* A hybrid vector for ligand-directed tumor targeting and molecular imaging. *Cell* **125**, 385–398 (2006).
- Nam, K. T. *et al.* Virus-enabled synthesis and assembly of nanowires for lithium ion battery electrodes. *Science* **312**, 885–888 (2006).
- Langer, R. & Tirrell, D. A. Designing materials for biology and medicine. *Nature* **428**, 487–492 (2004).
- Hautot, D. *et al.* Preliminary observation of elevated levels of nanocrystalline iron oxide in the basal ganglia of neuroferritinopathy patients. *Biochim. Biophys. Acta* **1772**, 21–25 (2007).
- Snyder, E. Y. *et al.* Multipotent neural cell lines can engraft & participate in development of mouse cerebellum. *Cell* **68**, 33–51 (1992).
- Wan, X., Li, Z. & Lubkin, S. R. Mechanics of mesenchymal contribution to clefting force in branching morphogenesis. *Biomech. Model. Mechanobiol.* **7**, 417–426 (2008).
- Csikasz-Nagy, A., Battogtokh, D., Chen, K. C., Novak, B. & Tyson, J. J. Analysis of a generic model of eukaryotic cell-cycle regulation. *Biophys. J.* **90**, 4361–4379 (2006).
- Ofek, G. *et al.* Matrix development in self-assembly of articular cartilage. *PLoS ONE* **3**, e2795 (2008).
- Bhowmick, D. A., Zhuang, Z., Wait, S. D. & Weil, R. J. A functional polymorphism in the EGF gene is found with increased frequency in glioblastoma multiforme patients and is associated with more aggressive disease. *Cancer Res.* **64**, 1220–1223 (2004).
- Chicoine, M. R. & Silbergeld, D. L. Mitogens as motogens. *J. Neurooncol.* **35**, 249–257 (1997).
- Georgescu, M. M., Kirsch, K. H., Akagi, T., Shishido, T. & Hanafusa, H. The tumor-suppressor activity of PTEN is regulated by its carboxyl-terminal region. *Proc. Natl Acad. Sci. USA* **96**, 10182–10187 (1999).

Acknowledgements

The authors would like to thank R.R. Brentani, N.R. Pellis and E.H. Sage for helpful discussions and K. Dunner Jr and D. Bier for technical assistance. G.R.S. was supported by the Odyssey Scholar Program of the University of Texas M.D. Anderson Cancer Center and by the Breast Cancer Research Program of the US Department of the Defense (DOD). D.J.S. received support from the National Science Foundation. T.C.K. received support from the David and Lucille Packard Foundation. W.A. and R.P. received support from the Gillson-Longenbaugh Foundation, the Marcus Foundation, AngelWorks, DOD, National Institutes of Health (NIH) and National Cancer Institute.

Author contributions

G.R.S., J.R.M., R.M.R., D.J.S., C.S.L., J.M., T.C.K., W.A. and R.P. conceived and designed the experiments. G.R.S., J.R.M., T.C.K., D.J.S., C.S.L., J.S.A. and J.M. performed the experiments. G.R.S., M.G.O., D.J.S., C.S.L., L.F.B., J.S.A., J.A.B., T.C.K., W.A. and R.P. analysed the data. R.M.R., M.M.G., J.A.B., J.G.G., T.C.K., W.A. and R.P. contributed materials and analysis tools. G.R.S., R.M.R., M.G.O., L.F.B., J.A.B., J.G.G., T.C.K., W.A. and R.P. co-wrote the paper.

Additional information

The authors declare competing financial interests: details accompany the paper at www.nature.com/naturenanotechnology. Supplementary information accompanies this paper at www.nature.com/naturenanotechnology. Reprints and permission information is available online at <http://npg.nature.com/reprintsandpermissions/>. Correspondence and requests for materials should be addressed to T.C.K., W.A. and R.P.